

Research on Adjustment Method of Power Flow Convergence Based on Planning Model

Hanwen Chen¹, Hua Zheng¹, Hui Li², Zhidong Wang², Jiaming Wang² and Shengyu Kuai³

¹North China Electric Power University, Beijing, China

²State Grid Economic and Technology Research Institute Co., Ltd, Beijing, China

³State Grid Anhui Electric Power Co., Ltd, Hefei, China

Email:chenhanwen1202@126.com

Abstract. Power flow calculation is an essential component of power network planning. The problem of its convergence adjustment has a great significance for research. This paper proposes a power flow convergence adjustment method based on a nonlinear programming model. It aims at the non-convergence problem of power flow calculation caused by reactive power imbalance. By introducing a set of slack variables into the AC/ DC power flow equations, the conventional power flow calculation is converted to a nonlinear programming model with the least square sum of slack value. Based on the characteristics of node slack value and its distribution law, the power flow reactive power adjustment method and its implementation steps are established, according to the electrical distance. The actual grid planning data of a certain place in China is simulated and calculated, which verifies the effectiveness and feasibility of the method.

1. Introduction

With the rapid construction of large-scale AC/DC hybrid power grid and the large-scale grid-connected access of renewable energy sources, the operating mode of large-scale interconnected power grids in China has become ever more complex and atypical. There are planned grid operation modes of large-scale renewable energy grid-connected and HVDC-containing. Thus, the number of non-convergence or poor convergence situations of conventional power flow models and algorithms is gradually increasing. However, when the power flow of the planned power grid does not converge, two ways of results can be observed. First, the existing power flow models and algorithms struggle to provide effective information for experienced planners to assist in adjustments. Also, the adjustment methods based on human experience of the increasingly complex large-scale planned power grid cannot provide the desirable outcome. Therefore, effectively adjusting the convergence of the power flow equations of the planned power grid is one of the most important issues to be solved in the field of large-scale power grid planning work.

The problem of power flow equations convergence can be roughly divided into two categories. First one would be power flow equations that have a solution, but, due to parameter errors or insufficient solving algorithms, are difficult or impossible to converge. The second one would be power flow equations that have no solutions. For this category the power flow calculation is not convergent. Aiming at the power flow equations in the first category, many global scholars mainly focus on improving the model and algorithm of various methods. Namely, the Newton-type method



[1-3], the optimal multiplier method [4-6], the nonlinear programming method, using optimization ideas [7-9], and the global convergence algorithm like the homotopy method [10-11]. Also, the provision of as much auxiliary adjustment information and adjustment methods as possible is aspired. The basic idea is to use the load down method to discover approximate solutions, analyze their results, and assist in adjusting the power flow. In general, the load down method requires constant and repeated attempts to adjust the system margin, load level, etc. This should continue until it recovers or approaches the original state. However, as the scale of the power grid increases, the number of reciprocal adjustments will drastically increase as well. This will make it difficult to meet the objective needs of the elaborate power grid planning work.

The causes of the power flow non-convergence can be divided into active and reactive power imbalance [15,16]. In the actual grid planning work, most of the planning power grid flow non-convergence is caused by reactive power imbalance. Very little of the power flow non-convergence is caused by active power imbalance. The adjustment of the power flow non-convergence, caused by the active power imbalance, is usually relatively simple and developed. The one caused by the reactive power imbalance is usually relatively difficult and inflexible.

Therefore, an auxiliary adjustment method based on planning model for power flow convergence is proposed in this paper. It aims solve the convergence difficulty problem of the planned power grid caused by reactive power imbalance. According to the characteristics of power grid planning, a corresponding nonlinear programming model and its algorithm are established. Then, the characteristics of node slack and their distribution rules in the calculation of planning models are analyzed. This is done while the power flow of the planned grid is not convergent. To solve the problem, a method to assist the adjustment of the convergence of the power flow and its implementation steps are established. The method is based on a nonlinear programming model. Finally, the actual power grid planning data of a certain place in China is applied and analyzed. The results of this analysis confirm the effectiveness of the method this paper presents.

2. Planning model

2.1. Model

The basic idea proposed by this paper is to slack the non-linear equations that need to be solved in the power flow calculation. A pair consisting of an active and a reactive power slack is introduced in each node. This transforms the power flow problem into the following nonlinear programming model.

$$\begin{cases} \min f(\varepsilon) = \sum \varepsilon^2 \\ \text{s.t.} & h(X) - \varepsilon = 0 \\ & \bar{g} \leq g(X) \leq \underline{g} \end{cases} \quad (1)$$

$g(X)$ represents inequality constraints, including:

$$\underline{U} \leq U(\Omega_{PQ}) \leq \bar{U} \quad (2)$$

$$\underline{P}_G \leq P_G(\Omega_{\text{Slack}}) \leq \bar{P}_G \quad (3)$$

$$\underline{Q}_G \leq Q_G(\Omega_{\text{Slack}} \cup \Omega_{PV}) \leq \bar{Q}_G \quad (4)$$

$$\underline{P}_d \leq U_d \cdot I_d \leq \bar{P}_d \quad (5)$$

$$\underline{U}_d \leq U_d \leq \bar{U}_d \quad (6)$$

$$\underline{I}_d \leq I_d \leq \bar{I}_d \quad (7)$$

$$\underline{K}_d \leq K_d \leq \bar{K}_d \quad (8)$$

$$\underline{A}_d \leq A_d \leq \bar{A}_d \quad (9)$$

$$\underline{\varphi}_d \leq \varphi_d \leq \bar{\varphi}_d \quad (10)$$

$H(x)=0$ is the power flow equation, U is the bus voltage amplitude; δ is the bus voltage phase angle; $U = U \angle \delta$ is the node complex voltage; P_G 、 Q_G is injection of active and reactive power of node; U_d is DC voltage of the converter station; I_d is DC current of the converter station; K_d is the tap position of the converter station rectifying transformer; $A_d \cos \theta_d$ is the cosine of the converter control angle of the converter station; φ_d is the power factor angle of the converter station; Ω_{PV} is the set of PV bus; Ω_{PQ} is the set of PQ bus; Ω_{Slack} is the set of balanced bus; $\bar{(\quad)}$ 、 $\underline{(\quad)}$ are the upper and lower limits of the corresponding variables.

2.2. Model solution

In this paper, the interior point method is used to solve the model. The slack variables is introduced to relax the equality and inequality constraints. Specific steps are presented as follows:

(1) By introducing slack variables l and u , inequality constraints can be converted to equality constraints as follows:

$$\begin{cases} g(X) - \underline{g} - l = 0 \\ g(X) - \bar{g} + u = 0 \end{cases} \quad (11)$$

(2) Definition of Lagrange function:

$$\begin{aligned} L(X, l, u, y, z, w, \varepsilon) = & \varepsilon^T \varepsilon - y^T (h(X) - \varepsilon) \\ & - z^T (g(X) - l - \underline{g}) - w^T (g(X) + u - \bar{g}) \\ & - \mu (\sum u_i + \sum l_i) \end{aligned} \quad (12)$$

Where y, z, w is a Lagrange multiplier.

(3) The first-order optimal conditions of the Lagrange function are presented as the following:

$$L_x = \nabla h(X)y + \nabla g(X)(z + w) = 0 \quad (13)$$

$$L_z = g(X) - l - \underline{g} = 0 \quad (14)$$

$$L_w = g(X) + u - \bar{g} = 0 \quad (15)$$

$$L_l^\mu = [l][z]e - \mu e = 0 \quad (16)$$

$$L_u^\mu = [u][w]e + \mu e = 0 \quad (17)$$

$$L_\varepsilon = 2\varepsilon + y = 0 \quad (18)$$

$$L_y = h(X) - \varepsilon = 0 \quad (19)$$

Where: e is the unit diagonal matrix; L_l^μ 、 L_u^μ are perturbation complementary conditions; \square indicates that the vector is converted to a diagonal matrix; μ is the interference factor.

Eliminating of ε from equations (18) and (19):

$$L_y = h(X) + 0.5y = 0 \quad (20)$$

(4) The correct equation was obtained by the irreducible conventional interior point method:

$$\begin{bmatrix} M & J(X)^T \\ J(X) & 0.5[e] \end{bmatrix} \begin{bmatrix} \Delta X \\ \Delta y \end{bmatrix} = - \begin{bmatrix} \psi \\ L_{y,0} \end{bmatrix} \quad (21)$$

Where:

$$M = F + \nabla g(X)([u]^{-1}[w] - [l]^{-1}[z])\nabla g(X)^T \quad (22)$$

$$F = \nabla^2 h(X)y + \nabla^2 g(X)(z + w) \quad (23)$$

$$J(X) = \nabla h(X)^T \quad (24)$$

$$\begin{aligned} \psi = \nabla h(X)y + \nabla g(X)([u]^{-1}[w]L_{w0} - \\ [l]^{-1}[z]L_{z0} - \mu([u]^{-1} - [l]^{-1})e) \end{aligned} \quad (25)$$

From equation (21) we can infer:

$$\Delta y = -2L_{y0} - 2J(X)\Delta X \quad (26)$$

Substituting equation (26) into equation (21) yields, we can get equation as follows:

$$(M - 2J(X)^T J(X))\Delta X = -\psi + 2J(X)^T L_{y0} \quad (27)$$

After the formula (27) is solved, the formula (26) is calculated. Then we can calculate the remaining correction according to the following equation:

$$\begin{cases} \Delta l = \nabla g(X)^T \Delta X + L_{z0} \\ \Delta u = -(\nabla g(X)^T \Delta X + L_{w0}) \\ \Delta z = -[l]^{-1}[z]\nabla g(X)^T \Delta X - [l]^{-1}([z]L_{z0} + L_{l0}^\mu) \\ \Delta u = [u]^{-1}[w]\nabla g(X)^T \Delta X + [u]^{-1}([w]L_{w0} - L_{u0}^\mu) \end{cases} \quad (28)$$

(5) By calculating the step size in the search direction and modifying X , l , u , y , z and w , ε can be obtained.

2.3. Analysing the slack characteristics

By formula (1) It can be seen that when the objective function value is 0, it means that the original equation group $H(x) = 0$ has a solution. Currently, the result of nonlinear programming is the same as the conventional power flow result. When the objective function value is not 0, the power flow equations are not convergent. At this time, the slack value of the ill-conditioned nodes and their neighboring nodes is not equal to 0. Therefore, by determining the amount of slack value, we can find out the surplus and deficiency of the power flow and its distribution.

When there is only active power imbalance, the active power slack value at the ill-conditioned nodes will be relatively large. At the same time, the active power slack value of the neighboring nodes around them will be relatively small. This means that the longer the electrical distance from the ill-conditioned nodes, the smaller active power slack value at the nodes will be.

When an active and a reactive power imbalance exist at the same time, the active power slack value at the active ill-conditioned nodes will be larger. The reactive power slack value at the reactive ill-conditioned nodes will also increase. The amount of the active and reactive power slack value at other nodes will be relatively small. This means that the longer the electrical distance from the ill-conditioned nodes, the smaller slack value at the nodes will be.

Therefore, When the power grid planning flow does not converge caused by reactive power imbalance, we can improve convergence by nonlinear programming results. The main basis of the method are the relationship and distribution law between the slack value at the ill-conditioned nodes and the power imbalance. By calculating the distribution cluster of the relaxation quantity in the nonlinear programming results, the reactive power compensation or adjustment of the nodes with the largest slack quantity in each cluster can be made. Thereby the convergence of the objective power flow could be improved.

3. Reactive power adjustment based on the minimization of the power flow

3.1. Implementation steps

The specific implementation steps are shown in Figure 1:

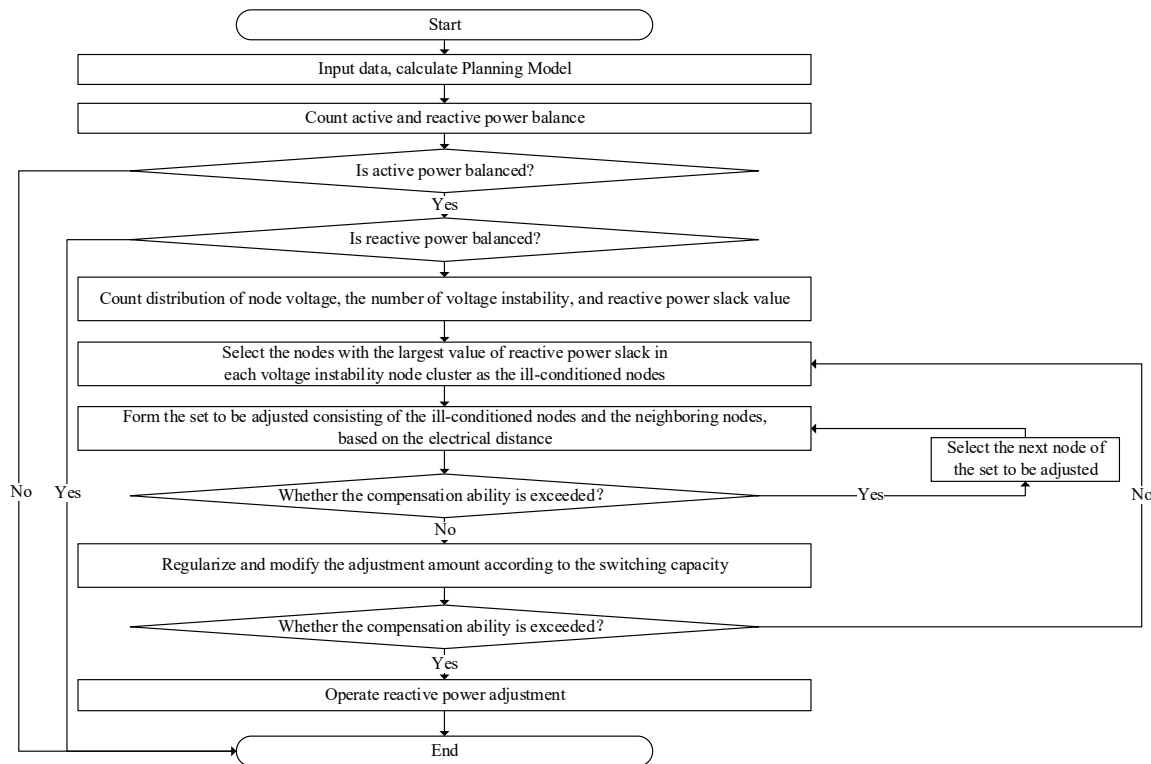


Figure 1. Flow chart of reactive power adjustment

- (1) Read power flow input data of the planned grid and solve the nonlinear equations;
- (2) Read the nonlinear programming result data to determine if the situation is an active or a reactive power imbalance;
- (3) If there is an active power imbalance, perform step (9);
- (4) If there is a reactive power imbalance, statistically calculate the number of voltage instability nodes and their reactive power slack value;
- (5) Select the nodes with the largest amount of reactive power slack value in each voltage instability node cluster as the ill-conditioned nodes. Their reactive power slack value is taken as the amount to be adjusted;
- (6) The electrical distance between other nodes and their ill nodes in each cluster is calculated in turn. According to the order of electrical distance from nearest to furthest, select the appropriate number of neighbouring nodes to form a set $\Omega_i = \{i, j_1, j_2, \dots, j_n\}$ to be adjusted, consisting of the ill-conditioned nodes, neighbouring nodes, and the amount to be adjusted;
- (7) In any set to be adjusted, according to the order of electrical distance from nearest to furthest, select the nodes to be adjusted in Ω_i . Determine the size relationship between the remaining adjustment of the nodes and their reactive equipment capacity. Then, calculate the amount of the adjustment until the remaining adjustment is 0;
- (8) Regulate and modify the amount of the last node adjustment in each set according to the minimum switching capacity of the reactive power device;
- (9) Output the result and exit the operation.

3.2. Node set to be adjusted

Assuming equal impedance $Z_{ij} = R_{ij} + jX_{ij}$ between nodes i and j , for a high-voltage power transmission network, because R_{ij} is far smaller than X_{ij} , the electrical distance can be further reduced to the reactance X_{ij} between two nodes. The reactive power transmitted from the node i to j satisfies the following approximate relationship:

$$Q_{ij} \approx \frac{U_i(U_i - U_j)}{X_{ij}} \quad (29)$$

According to the above formula, the reactive power transmitted between nodes i and j is inversely proportional to the equivalent reactance X_{ij} between the two nodes. This means that the shorter the electrical distance from the node to be ill, the more obvious the effect of the reactive power and voltage support for the ill-conditioned node.

Therefore, centred on the ill-conditioned nodes, according to the network topology, the electrical distance between the ill-conditioned node and the neighbouring nodes is calculated respectively. The neighbouring nodes constitute the set Ω_i to be adjusted. After sorting the electrical distance from nearest to furthest, we calculate the cumulative capacity sum $Q_{shunt}(\Omega_i, m)$ of the first m nodes to be adjusted in Ω_i in turn. When the cumulative capacity sum $Q_{equip}(\Omega_i, m)$ to be adjusted is less than or equal to the maximum capacity sum of the reactive power device of the first m nodes, the first m nodes will form a transfer adjustment node set $T_i = \{i, j_1, j_2, \dots, j_{m-1}\}$. If a node i does not have a reactive power device, its reactive device capacity $Q_{equip-i}$ will be 0.

When $m=n$, the remaining adjustment is not greater than 0. This means that when the node Ω_i set to be adjusted cannot satisfy the adjustment requirement at this time, the network topology structure should be extended outward to increase the scale of the node Ω_i set to be adjusted.

3.3. Transfer adjustment node compensation amount

For the set T_i of transfer adjustment nodes consisting of m nodes, the adjustment amounts of the first node to node $m-1$ are equal to the maximum capacity of the reactive devices of the respective nodes. The adjustment amount of the node m is the algebraic difference between the cumulative maximum capacity sum of the reactive power device of the former $m-1$ nodes and the adjustment amount of this cluster.

3.4. Regularization and correction of Adjustments

In the actual power grid, most of reactive equipment has a limit of minimum switching capacity. Therefore, the node m needs to undergo correction processing.

Assuming that the switching combination capacity of reactive power equipment of node i is $C_{Q_i} = \{Q_{i-1}, Q_{i-2}, \dots, Q_{i-n}\}$, the adjustment amount of node i is Q_i , between the value Q_{i-1} and Q_{i-2} . The value should be the closest value to Q_i in the set C_{Q_i} , so if it is $Q_i < 1/2(Q_{i-1} + Q_{i-2})$, that is $Q_i = Q_{i-1}$, otherwise $Q_i = Q_{i-2}$.

4. Example analysis

To carry out a simulation analysis necessary for this paper, MATLAB and PSD-BPA power system analysis software was used. The analysis was based on a planned power network of a certain place in Northwest China. This power grid contains 328 nodes. This includes 53 generator nodes, installed capacity 26020 MW, 275 load nodes, active load 23250 MW, 325 AC lines, and 113 transformers. To simplify the analysis, the reactive power compensation capacity of each non-generator node is 30 MVar. The single group switching capacity is 5 MVar.

By PSD-BPA calculation, the power flow is currently not convergent. In this paper, the power flow model and algorithm were used to recalculate the method. Using the results of nonlinear programming, it was found that the method is active power balance and reactive power imbalance. Among them, the iteration number initial value $k=0$, maximum iteration number $K_{\max}=100$, central parameter $\sigma \in (0,1]$, admissible error $\varepsilon = 10^{-3}$, and select slack variables $[l, u]^T \geq 0$.

4.1. Example result

The minimum value of the objective function is 3556.8 after 29 iterations. Figure 2 is the slack distribution of nodes in the power flow results. Fig 3 is the distribution map of reactive slack value of each node. All the reactive power units in this example are MVar. For the convenience of narration, no unit is added in the subsequent part of the calculation example.

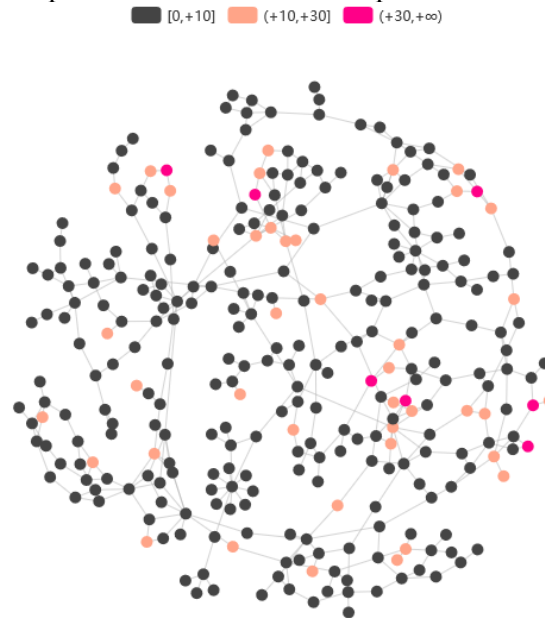


Figure 2. Distribution figure of reactive power slack node

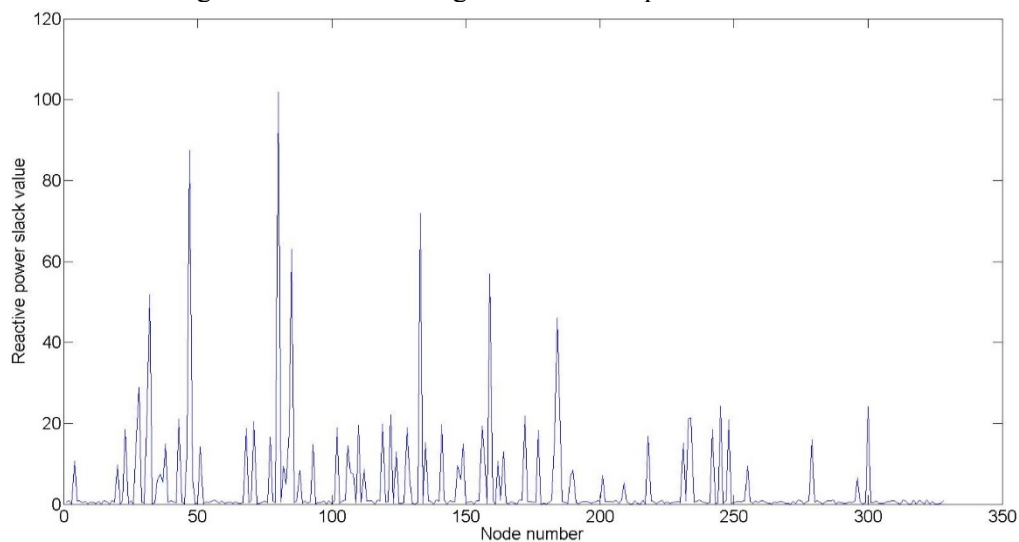


Figure 3. Distribution figure of reactive power slack value

From Figure 2 and figure 3, the reactive power slack value of 280 nodes is between [0 and +10], accounting for 85.37%. The reactive power slack value of 41 nodes is (10, +30], accounting for 12.5%, and the reactive power slack value of 7 nodes is greater than that of +30, accounting for 2.13%. Through network topology analysis, we can see that there are 5 ill conditioned clusters, which contain all the 7 largest slack nodes.

Table 1. Table of nodes whose value of reactive residual is greater than 30

Node number	bus-32	bus-47	bus-80	bus-85
Reactive power relaxation	51.82	87.51	101.84	62.93
Node number	bus-133	bus-159	bus-184	-
Reactive power relaxation	71.79	56.91	46.01	-

4.2. Analysis of reactive power adjustment

To verify the effectiveness of this method, 2 representative clusters are selected for detailed analysis:

(1) With bus-32 as the pathological node, the reactive power should be adjusted to exceed its reactive power capacity. The reactive power capacity of the surrounding nodes will be sufficient.

(2) With bus-80 as the pathological node, the reactive power should be adjusted to exceed its reactive power capacity. The reactive power capacity of the surrounding nodes is not sufficient.

Table 2 lists the data of ill posed nodes and their adjacent nodes in the above 2 representative clusters.

Table 2. Data tables of representing nodes and their adjacent nodes

	Pending node			Adjacent nodes
Node number	bus-32	bus-31	bus-35	bus-37
Reactive power relaxation	51.82	18.71	6.04	5.41
Node number	bus-80	bus-82	bus-83	-
Reactive power relaxation	101.84	9.39	5.02	-

The cluster to be adjusted is read into the calculation module of reactive power transfer adjustment, and the output is shown in Table 3. Analysis of the reactive power data before and after the transfer adjustment:

(1) For bus-32, to adjust the amount of 51.82 MVar, according to the maximum reactive capacity of its actual configuration is 30 MVar, so 21.82 MVar must be transferred and adjusted. By calculating the electrical distance, we form the set to be adjusted to {bus-32, bus-31, bus-37, bus-35}. After calculation, the node bus-37 satisfies the adjusting requirements, and the transfer adjustment node set is {bus-32, bus-31, bus-37}, so the reactive power adjustment of node bus-32 and bus-31 are 30 MVar, the maximum capacity of reactive power equipment on the node. Then the reactive power adjustment of node bus-37 is equal to the residual adjustment 15.94 MVar. The node bus-35 remains unchanged.

(2) For bus-80, the adjusted capacity is 101.84 MVar, and the maximum reactive power capacity is 30 MVar according to its actual configuration, so it is necessary to transfer and adjust 71.84 MVar. By calculating the electrical distance, we form the set to be adjusted to {bus-80, bus-82, bus-83, bus-79}. After calculation, the node bus-79 satisfies the adjustment requirement, and the transfer adjustment node is {bus-82, bus-83, bus-79}, so the reactive power adjustment of the node is the maximum capacity of reactive power on the node, all of which are 30 MVar. The reactive power adjustment of node bus-79 is equal to the residual adjustment amount 26.66 MVar.

Table 3. Table of reactive power of nodes after reactive power transfer and adjust

Before adjustment	After adjustment	Adjacent nodes			Extension node
bus-32	bus-32	bus-31	bus-37	bus-35	-
51.82	30.00	30.00	15.94	0	-
bus-47	bus-47	bus-38	bus-46	bus-48	bus-37
87.51	30.00	30.00	30.00	30.00	6.84

Before adjustment	After adjustment	Adjacent nodes			Extension node
bus-80	bus-80	bus-82	bus-83	bus-79	-
101.84	30.00	30.00	30.00	26.66	-
bus-85	bus-85	bus-83	bus-88	bus-233	bus-81
62.93	30.00	30.00	30.00	30.00	2.77
bus-133	bus-133	bus-135	bus-162	bus-134	-
71.79	30.00	30.00	30.00	7.90	-
bus-159	bus-159	bus-124	bus-157	-	-
56.91	30.00	4.86	30.00	-	-
bus-184	bus-184	bus-172	bus-183	bus-185	-
46.01	30.00	21.83	30.00	26.07	-

After adjusting the amount of the transfer adjustment node, the adjustment amount is modified and corrected. The result is shown in Figure 4. The "Shunt admittance reactive power load" in the corresponding node card in the data file of the PSD-BPA is modified to the normalized corrected data. The PSD-BPA calculation is recalled, power flow is converged, and the voltage of each node in the tidal current is shown as shown in Figure 5.

4.3. Result analysis

As shown in table 4, after reactive power adjustment, the distribution of node voltage is slightly worse than the direct local adjustment compensation. The number of nodes in voltage 0.70-0.85, 0.85-0.95 and 1.05-1.10 increases by 0.61%, 1.52%, 0.30% respectively. The number of nodes in voltage 0.95-1.05 is reduced by 2.44%. After the reactive power transfer adjustment, the voltage qualification rate has decreased, but the deviation is less than 5%, and the power flow is convergent. Compared with the method of local adjustment, this method is seen to have more practical value.

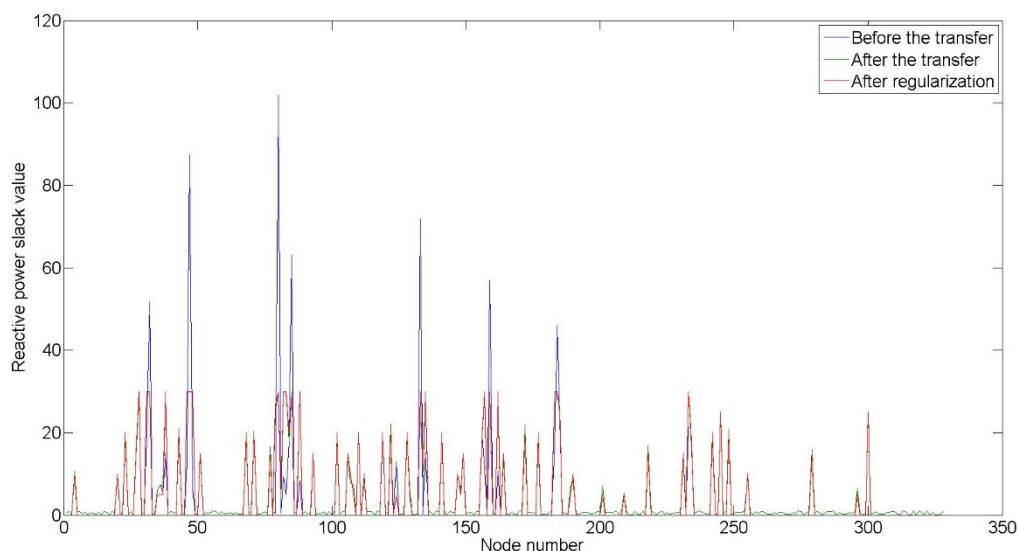


Figure 4. Reactive power adjustment value of each node before and after transfer

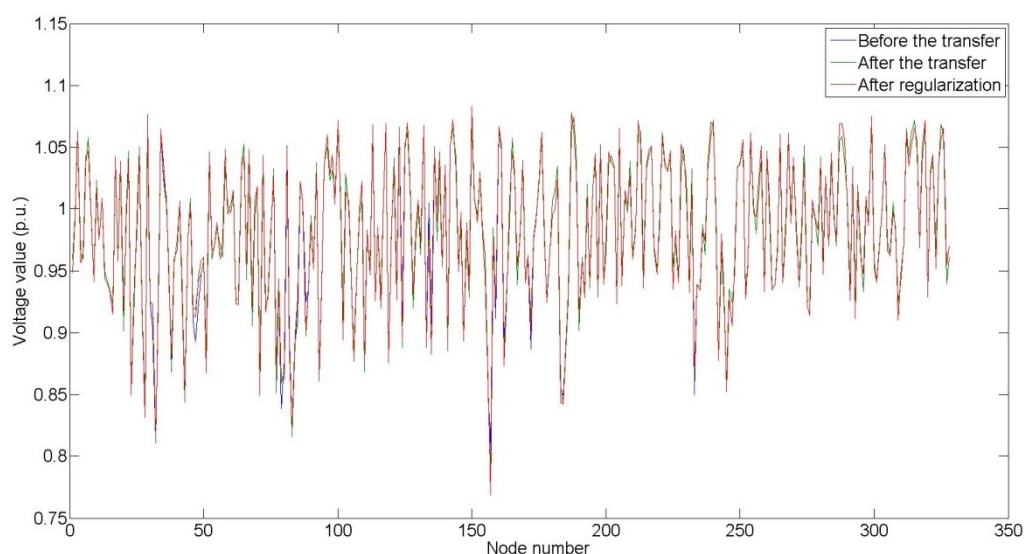


Figure 5. Voltage contrast diagram of each node before and after transfer

Table 4. Distribution of voltage at each node before and after reactive power adjustment

Range	0.80-0.85	0.85-0.95	0.95-1.05	1.05-1.10
Prefix transfer	2.13%	30.18%	54.27%	13.41%
Post transfer	2.74%	31.10%	52.74%	13.41%
After regulation	2.74%	31.71%	51.83%	13.72%

5. Epilogue

In view of the power flow convergence difficulty, caused by the reactive power imbalance, the result of nonlinear programming model can provide the auxiliary information and the adjustment method required to adjust the convergence of the power flow. It is a new solution and a realization scheme. To some extent, the problem of auxiliary adjustment information shortage and inefficient traditional adjustment methods is solved when the large-scale AC / DC power network does not converge. Through the example of an actual power grid planning data in China, the method that regard nodes with larger slack value in the grid mode as ill conditioned nodes to transfer and adjust can better meet the actual situation of the power grid planning. The effects on the results can be acknowledged within the acceptable range. At present, this paper only employs the reactive power slack value to solve the power flow convergence difficulty problem caused by the reactive power imbalance. Further study is necessary to discover how to make better use of the nonlinear programming results information and explore a more efficient power flow aided optimization and adjustment method.

References

- [1] Sun Q, Chen H, Yang J, et al 2014 Analysis on Convergence of Newton-like Power Flow Algorithm *Proceeding of the CSEE* **34** 2196-200
- [2] Zhang F, Cheng C S 2002 A modified Newton method for radial distribution system power flow analysis *IEEE Transactions on Power Systems* **1** 389-97
- [3] ZHANG Xinyi, HAN Xueshan, SUN Donglei, et al 2017 A Hybrid AC/DC Grid Power Flow Algorithm With Node Voltages as State Variables *Power System Technology* **5** 1484-90
- [4] Hu Zechun, Wang Xifan 2006 Determination of Static Voltage Collapse Critical Point Based

- on Load Flow Method with Optimal Multiplier *Automation of Electric Power Systems* **6** 6-11
- [5] Hu Zechun ,Yan Zheng 2009 Application of Newton Load Flow Methods with Optimal Multiplier for AC/DC Power Systems *Automation of Electric Power Systems* **9** 26-31
- [6] Goswami S K, Acharjee P 2010 Multiple low voltage power flow solutions using hybrid PSO and optimal multiplier method *Expert Systems with Applications* **37** 2473-6
- [7] QIN Zhijun HOU Yunhe Felix F Wu 2011 Practical Model for Large-scale AC-DC System Power Flow Calculation *Proceeding of the CSEE* **10** 95-101
- [8] ZHENG Hua, LI Hui, XIAO Jinyu, et al 2015 Research on Model and Algorithm for Optimal Power Flow of Large-scale High Voltage Direct Current Transmission System *Proceedings of the CSEE* **9** 2162-9
- [9] WU Weiping, HU Zechun, SONG yet al 2016 Hybrid Optimization of Optimal Power Flow by Combining the Semidefinite Programming and Nonlinear Programming *Proceedings of the CSEE* **14** 3829-36
- [10] Chiang H D, Zhao T Q, Deng J J, et al 2013 Homotopy-Enhanced Power Flow Methods for General Distribution Networks With Distributed Generators *IEEE Transactions on Power Systems* **1** 93-100
- [11] Mehta D, Nguyen H D, Turitsyn K 2016 Numerical polynomial homotopy continuation method to locate all the power flow solutions *Iet Generation Transmission & Distribution* **12** 2972-80
- [12] Canizares C A, Alvarado F L 2002 Point of collapse and continuation methods for large AC/DC systems *IEEE Transactions on Power Systems* **1** 1-8
- [13] Capitanescu F, Wehenkel L 2010 Sensitivity-Based Approaches for Handling Discrete Variables in Optimal Power Flow Computations *IEEE Transactions on Power Systems* **4** 1780-9
- [14] Han Y, Rosehart W D 2012 An Optimal Power Flow Algorithm to Achieve Robust Operation Considering Load and Renewable Generation Uncertainties *IEEE Transactions on Power Systems* **4** 1808-17
- [15] LI Zhihuan,HAN Yunfei,SU Yinsheng, et al 2015 A Convergence Adjustment Method of Power Flow Based on Node Type Switching *Automation of Electric Power Systems* **7** 188-93
- [16] YAN Zheng, FAN Xiang, ZHAO Wenkai,et al 2015 Improving the Convergence of Power Flow Calculation by a Self-adaptive Levenberg-marquardt method *Proceedings of the CSEE* **8** 1909-18